Proceedings of the
46th IEEE Conference on Decision and Control
New Orleans, LA, USA, Dec. 12-14, 2007

Energy-balancing cooperative strategies for sensor deployment

Andrew Kwok and Sonia Martínez

***Abstract*— This paper proposes power-aware coverage algorithms for mobile sensor networks. In order to balance the energy expenditure across the network and make nodes with high power compensate for those with low power, we propose two modified Lloyd-like algorithms. The first limits the velocity at which each node can travel, while the second incorporates a new definition of region of dominance depending on energy content. We introduce a power aware aggregate cost function and analyze the algorithms performance with regards to it. Various simulations illustrate this performance and compare both algorithms.**

I. Introduction

Mobile and static sensor networks hold the promise to impact a large number of applications for exploration, environmental monitoring, safety and recovery operations. It is envisioned that next network generations will make use of small low power mobile devices that operate in a distributed manner. Due to their modest sizes and weights, these systems will have limited resources to put into their different communication, computation and motion sub capabilities. Power management becomes then a crucial issue for these systems.

Motion coordination algorithms being proposed for multi-vehicle systems should also include power considerations. In particular, power redistribution over the multi-vehicle system could be employed together with coordination plans to diminish the possibilities of single agent failure. In this regard, the overall *sensor network lifetime* of a coordination algorithm or, the operational time until a first agent runs out of batteries, could be considered as another robustness measure for these distributed systems. Network-wide energy-minimizing policies can, combined with individual energy-minimizing laws, further contribute to limit the overall power consumption.

The topic of power-aware algorithms is the subject of extensive research in the areas of static sensor networks and mobile middleware, see e.g., [1], [2], [3], [4], [5]. To the best of our knowledge, there has been limited treatment of power-awareness in the cooperative control area, see [6], [7]. Related work is that where distributed Receding Horizon strategies have been investigated to plan optimal local vehicle trajectories or optimization of formations in multi-vehicle systems, see e.g., [8], [9], [10]. Power reallocation would be complementary to an approach that proposes global optimal energy motion coordination schemes.

A. Kwok is at the department of Mechanical and Aerospace Engineering, Univ. of California, San Diego, 9500 Gilman Dr, La Jolla CA, 92093 ankwok@ucsd.edu

S. Martínez is at the department of Mechanical and Aerospace Engineering, Univ. of California, San Diego, 9500 Gilman Dr, La Jolla CA, 92093 soniamd@ucsd.edu

This paper is a first attempt to analytically address the power-aware question in the context of coverage problems. Thus we propose two power-aware Lloyd-like algorithms for the coverage of the convex region of an N-dimensional space. Our objective is to determine algorithms that (i) augment the network lifetime, and (ii) achieve task redistribution according to the energy content of agents. The first algorithm includes agents' energy dynamics in the usual Lloyd algorithm, which guarantees that agents do not run out of energy. The second algorithm makes an additional use of a power-aware partition of the space to redistribute the coverage load across the network. Unlike the tessellations used to account for the cost of a location in e.g. market area analysis in locational optimization, here we use the *power weighted metric* tessellation. This enables the definition of simpler, convex regions of dominance for each agent, which results in faster computations. We show that the second proposed algorithm is gradient descent with respect to a modified power-aware coverage cost function, and we compare both algorithms in simulation. As expected, simulations indicate that the second algorithm more effectively redistributes the dominance region assigned to each agent depending on their power.

The paper is organized as follows. In Section II we recall useful concepts from locational optimization and introduce generalized Voronoi partitions associated with weighted metrics. In Section III, we develop a power-aware partition with its associated cost function. We introduce two power-aware algorithms in Section IV and analyze them from the point of view of a power-aware coverage cost function. Section V discusses the performance of the algorithms in simulation. Finally we point out lines for future research in Section VI.

II. Preliminaries and notation

In this section we review some known facts about Voronoi partitions and locational optimization problems defined using general metric functions. Our main reference is [11] for spatial tessellations, and [12] for an introduction to the discipline of locational optimization.

A. Generalized Voronoi partitions

Let Q be a convex polytope in $\mathbb{R}^N$ including its interior, and let $\|\cdot\|$ denote the Euclidean norm. We will use $\mathbb{R}_{\geq 0}$ to denote the set of positive real numbers. We denote the interior of Q by $\text{Int}(Q)$. We call a map $\phi : Q \to \mathbb{R}_{\geq 0}$ a *distribution density function* if it represents a measure of a priori known information that some event takes place over Q. Equivalently, we can consider Q to be the bounded support of the function ϕ. Let $P = (p_1, \dots, p_n) \in Q^n$ be the *location*

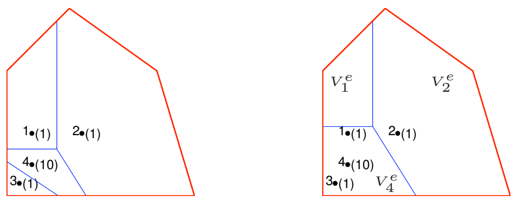

Fig. 1. Comparison between ordinary Voronoi regions (left) and power-weighted regions (right). Agent weights are in parenthesis. Note that, in the power-aware regions, agent 1 is not in its region of dominance and that agent 3 has no region of dominance in Q.

of n sensors, each moving in the space Q. Along the paper, we interchangeably refer to the elements of the network as sensors, agents, vehicles, or robots. Because of noise and loss of resolution, the *sensing performance* at point q taken from the ith sensor at the position p_i degrades with the distance $\|q-p_i\|$ between q and p_i; we can describe this degradation with a non-decreasing differentiable function $f : \mathbb{R}_{\geq 0} \to \mathbb{R}_{\geq 0}$. Thus, $f(\|q-p_i\|)$ provides a quantitative assessment of how poor the sensing performance is.

A *partition* of $\mathbb{R}^N$ is a collection of n polytopes $\mathcal{A} = \{A_1, \dots, A_n\}$ with disjoint interiors whose union is $\mathbb{R}^N$. The ordinary Voronoi partition of $\mathbb{R}^N$ generated by P is $\mathcal{V}(P) = \{V(p_1), \dots, V(p_n)\}$, where for $i \in \{1, \dots, n\}$,

$$V(p_i) = \{q \in \mathbb{R}^N \mid \|q-p_i\| \leq \|q-p_j\|, \ \ \forall j \neq i\}.$$

When is clear from the context we will use the shorthand notation $V_i = V(p_i)$. The *mass* and the *centroid* of the Voronoi region V_i, $i \in \{1, \dots, n\}$ are defined as:

$$M_{V_i} = \int_{V_i} \phi(q)dq\,, \qquad C_{V_i} = \frac{1}{M_{V_i}} \int_{V_i} q\phi(q)dq\,. \tag{1}$$

If Q is the bounded support of ϕ, then $M_{V_i} < +\infty$ and $C_{V_i} \in \text{Int}(Q)$; see [13]. When $M_{V_i} = 0$, then we will consider any point in $\mathbb{R}^N$ as a centroid for V_i. When two Voronoi regions V_i and V_j are adjacent (i.e., they share an edge), p_i is called a *Voronoi neighbor* of p_j. The set of indices of the Voronoi neighbors of p_i is denoted by $\mathcal{N}_i$. Clearly, $j \in \mathcal{N}_i$ if and only if $i \in \mathcal{N}_j$. We also define the (i,j) face as $\Delta_{ij} = V_i \cap V_j$.

With the introduction of agent weighting, the corresponding generalized Voronoi diagram must use *weighted metrics*. The following weighted metrics yield non-equivalent Voronoi partitions. The *multiplicatively weighted*, *additively weighted*, and *power metrics* [11] are:

$$\begin{aligned} d_w^{\mathrm{M}}(q,p) &= \frac{1}{w}\|p-q\|\,, \\ d_w^{\mathrm{A}}(q,p) &= \|q-p\| - w\,, \\ d_w^{\mathrm{P}}(q,p) &= \|q-p\|^2 - w\,, \end{aligned}$$

for any $q, p \in \mathbb{R}^N$. The generalized Voronoi regions associated with these metrics are non-equivalent and have very different characteristics. In particular, the generalized Voronoi regions associated with d_w^{M} could be non-convex, and may have holes or disconnected boundaries. Conversely, the regions associated with d_w^{A} may be empty, are star-shaped with respect to the generator, and the boundaries are defined by either hyperbolic arcs or a straight line segments. Regions associated with d_w^{P} are, notably, convex polygons. Generators, however, might not be in their regions.

We will make use of the power metric to model the energy content of a set of mobile sensors. This choice is motivated by the great computational simplification provided when dealing with convex polytopes. We denote the partition created by the power metric as $\mathcal{V}^e(P) = \{V^e(p_1), \dots, V^e(p_n)\}$ where for each $i \in \{1, \dots, n\}$,

$$V^e(p_i) = \{q \in \mathbb{R}^N \mid d_{w_i}^{\mathrm{P}}(q,p_i) \leq d_{w_j}^{\mathrm{P}}(q,p_j)\,,\ \forall j \neq i\}\,.$$

When it is clear from the context, we will use the shorthand notation $V_i^e = V^e(p_i)$. Defined in an analogous manner to (1), $M_{V_i^e}$ and $C_{V_i^e}$ will denote the mass and the centroid of the generalized Voronoi region V_i^e. When $M_{V_i^e} = 0$, then we will consider that any point in $\mathbb{R}^N$ is a centroid for V_i^e. Similarly as before, each generalized Voronoi region V_i^e generated by p_i has a set of neighbors $\mathcal{N}_i^e$, and a pair of neighbors under the power metric share the face $\Delta_{ij}^e = V_i^e \cap V_j^e$.

Figure 1 illustrates the difference between Voronoi and generalized Voronoi regions, when these are intersected with a convex polytope Q. In the figure, $Q \subset \mathbb{R}^2$, where the vertices of Q are at $(0,0), (15,0), (12,10), (5,15), (0,10)$.

B. Locational optimization problems

Locational optimization problems consider the minimization of the following type of cost functions:

$$\mathcal{H}(P, \mathcal{A}) = \sum_{i=1}^{n} \int_{A_i} f(\|q-p_i\|)\phi(q)dq\,. \tag{2}$$

Minimization is understood with respect to $P \in \mathbb{R}^{Nn}$ and a partition $\mathcal{A}$.

This definition assumes that sensors are identical, or homogeneous. In some instances, it is more appropriate to consider that agents do not have the same capabilities. This can be reflected by the introduction of weights.

Let $W = (w_1, \dots, w_n) \in \mathbb{R}^n$ be a tuple of real parameters which represent some weights associated with each of the locations $P = (p_1, \dots, p_n)$, respectively. The cost functions in (2) can then be extended to:

$$\mathcal{H}_e(P, W, \mathcal{A}) = \sum_{i=1}^{n} \int_{A_i} f(d_{w_i}(q,p_i))\phi(q)dq\,, \tag{3}$$

where $d_w : \mathbb{R}^N \times \mathbb{R}^N \to \mathbb{R}_{\geq 0}$ is a weighted metric for some $w \in \mathbb{R}$.

III. Power-aware coverage metric

Here we introduce a power-metric cost function to assess the coverage provided by a mobile network. The power content of vehicles will be specified through the inclusion of a certain weight in measuring the distance to points in the space.

Consider a tuple of points $(p_1, \ldots, p_n)$ representing the positions of n identical sensors moving in Q. Assume that each p_i has an "energy content" quantified by $E_i \in [0, E] \subseteq \mathbb{R}$ for all $i \in \{1, \ldots, n\}$, where E represents the maximum battery capacity of each sensor.

Let $E - E_i$ be the power reserve of agent $i \in \{1, \ldots, n\}$, which defines the weight $e_i = E_i - E$, $i \in \{1, \ldots, n\}$. Then, the cost of a point p_i to cover a point of the space $q \in Q$ becomes:

$$d^{\mathrm{P}}_{e_i}(q, p_i) = \|q - p_i\|^2 - e_i = \|q - p_i\|^2 + (E - E_i),$$

for all $i \in \{1, \ldots, n\}$. In this way, $d^{\mathrm{P}}_{e_i}(q, p_i) \geq 0$ for all $i \in \{1, \ldots, n\}$. Observe also that we can interpret $d^{\mathrm{P}}_{e_i}$ as the distance between extended states (q, E) and (p_i, E_i), $i \in \{1, \ldots, n\}$.

In other words, the cost will depend on how physically close the sensor p_i is to q and on how "charged" it is; i.e., how close E_i is to the maximum battery capacity E. Let $\mathcal{E} = (e_1, \ldots, e_n)$, then from (3) we obtain a cost that takes into account that sensors are not equal:

$$\begin{aligned}\mathcal{H}_e(P, \mathcal{E}, \mathcal{V}^e(P)) &= \sum_{i=1}^{n} \int_{V_i^e} d^{\mathrm{P}}_{e_i}(q, p_i)\phi(q)dq \\ &= \int_Q \min_{i \in \{1,\ldots,n\}} f(d^{\mathrm{P}}_{e_i}(q, p_i))\phi(q)dq\,. \end{aligned} \quad (4)$$

Roughly speaking, (4) is the expected minimum distance of points $q \in Q$ to the set of sensors $p_1, \ldots, p_n$, where the distance includes energy considerations. For example, a point equidistant from two sensors will fall in the region of dominance of the one with greater energy.

Remark 1: Another weighted distance metric could be

$$d^{\mathrm{P}}_{E_i}(q, p_i) = \|q - p_i\|^2 - E_i^2\,.$$

This would still produce a power-weighted Voronoi diagram, but the derivation for the above metric is more involved. The above result does not, however, affect the focus of this paper, which is introducing power considerations during the execution of coverage algorithms. •

Function (4) naturally extends the cost:

$$\mathcal{H}(P, \mathcal{V}(P)) = \int_Q \min_{i \in \{1,\ldots,n\}} f(\|q - p_i\|)\phi(q)dq\,. \quad (5)$$

considered in [14]. Note also that in the limit case for which the energy available to each agent E is very large; i.e., for which any finite-length motion will not substantially decrease it, then the minimization of (4) is equivalent to the minimization of the usual cost (5).

To see this, suppose that E_i is specified as a time dependent function $E_i : \mathbb{R} \to [0, E]$, for $i \in \{1, \ldots, n\}$. Suppose $E_i(t) \approx E_j(t)$ after a finite time t. This implies:

$$\begin{aligned}&d^{\mathrm{P}}_{e_i}(q, p_i) \leq d^{\mathrm{P}}_{e_j}(q, p_j) \\ &\quad\iff \|q - p_i(t)\|^2 \leq \|q - p_j(t)\|^2\,, \quad \forall\, q \in Q\,.\end{aligned}$$

Then $V_i(t) \approx V_i^e(t)$ for all $i \in \{1, \ldots, n\}$ and minimizing $\mathcal{H}_e$ is equivalent to minimizing $\mathcal{H}$.

In any case, the minimization cost $\mathcal{H}_e$ leads to final configurations for coverage with a more balanced region assignment based on the power content of agents.

IV. Power-aware gradient descent flows

In this section we present power-aware control algorithms that minimize $\mathcal{H}$ in (5) and $\mathcal{H}_e$ (4). In the following we assume that the motion of each sensor can be fully controlled as $\dot{p}_i = u_i$, $i \in \{1, \ldots, n\}$ and we consider the energy dynamics:

$$\dot{E}_i = \begin{cases} -u_i^2\,, & \text{if } E_i \geq 0\,, \\ 0\,, & \text{if } E_i = 0\,. \end{cases} \quad (6)$$

Lloyd's algorithm, see [14], with the additional energy dynamics is then expressed as:

$$\begin{aligned}\dot{p}_i &= -\mathrm{sat}(p_i - C_{V_i})\,, \\ \dot{E}_i &= -\|\mathrm{sat}(p_i - C_{V_i})\|^2\,,\end{aligned} \quad (7)$$

where

$$\mathrm{sat}(p_i - C_{V_i}) = \begin{cases} p_i - C_{V_i}\,, & \text{if } \|p_i - C_{V_i}\| \leq 1\,, \\ \dfrac{p_i - C_{V_i}}{\|p_i - C_{V_i}\|}\,, & \text{if } \|p_i - C_{V_i}\| > 1\,. \end{cases}$$

When energy restrictions are not considered, Lloyd's algorithm is a gradient descent algorithm for $\mathcal{H}$, see [14]. A continuous, power-aware version of this algorithm could be defined as follows:

$$\begin{aligned}\dot{p}_i &= -k(E_i)\,\mathrm{sat}(p_i - C_{V_i})\,, \\ \dot{E}_i &= -k(E_i)^2\,\|\mathrm{sat}(p_i - C_{V_i})\|^2\,,\end{aligned} \quad (8)$$

where $k : [0, E] \to [0, 1]$ is such that $k(x) = \dfrac{x}{E}$. The introduction of $k(E_i)$ limits velocity based on the current energy level E_i.

Both algorithms (7) and (8) are gradient descent algorithms for the ordinary cost function $\mathcal{H}$. However, they are not gradient descent algorithms for the weighted cost (4). Consider instead:

$$\begin{aligned}\dot{p}_i &= -k(E_i)\,\mathrm{sat}(p_i - C_{V_i^e})\,, \\ \dot{E}_i &= -k(E_i)^2(t)\,\|\mathrm{sat}(p_i - C_{V_i^e})\|^2\,.\end{aligned} \quad (9)$$

Observe that when $V_i^e \cap Q = \emptyset$, then $M_{V_i^e} = 0$ and we can consider that $p_i = C_{V_i^e}$.

Lemma 2: The choice of the $k(E_i)$ function in the dynamics (8) and (9) guarantees that E_i only approaches zero asymptotically.

Proof: We prove this fact only for (8), since the proof for (9) is analogous. From (8), we have that:

$$\dot{E}_i = -\frac{E_i^2}{E^2}\|\,\mathrm{sat}(p_i - C_{V_i})\|^2,$$

which implies that

$$E_i(t) = \frac{E^2}{1 + E\int_0^t \|\,\mathrm{sat}(p_i - C_{V_i})\|^2(s)\,ds}\,,$$

that is, $E_i(t)$ decreases with time, but in the worst case it will be zero only at infinity. ■

In order to prove that algorithm (9) is a gradient descent algorithm for $\mathcal{H}_e$, we first compute the gradient and Lie derivative of (4).

Theorem 3: Let $\mathcal{H}_e$ be given by (4). Consider a general vector field $X = (X_1, \dots, X_n)$, where

$$X_i = (X_{p_i}, X_{E_i}) : Q \times [0, E] \to \mathbb{R}^N \times \mathbb{R}\,, \tag{10}$$

for all $i \in \{1, \dots, n\}$. Then, the Lie derivative of $\mathcal{H}_e$ with respect to X is given as:

$$\mathcal{L}_X \mathcal{H}_e = \sum_{j=1}^{n} \Big(2M_{V_j^e}(p_j - C_{V_j^e})X_{p_j} - M_{V_j^e} X_{E_i} \Big)\,. \tag{11}$$

Proof: Since the density function ϕ has bounded support on Q, we can consider that the integration domain in $\mathcal{H}_e$ is $\mathbb{R}^N$. All the subsequent computations are done with this simplification. The Lie derivative of $\mathcal{H}_e$ with respect to X becomes:

$$\sum_{i,j=1}^{n} \Big[X_{p_j} \frac{\partial}{\partial p_j} \int_{V_j^e} \big(\|q - p_i\|^2 + (E - E_i)\big)\phi(q)dq + X_{E_j} \frac{\partial}{\partial E_j} \int_{V_i^e} \big(\|q - p_i\|^2 + (E - E_i)\big)\phi(q)dq \Big]\,.$$

Since the regions V_i^e are convex, we can compute the foregoing partial derivatives via the Conservation of Mass law [13]:

$$\frac{d}{dx} \int_{\Omega(x)} \varphi(q, x)dq = \int_{\Omega(x)} \frac{d\varphi(q, x)}{dx} dq + \int_{\partial\Omega(x)} \varphi(\gamma, x) n^t(\gamma) \frac{\partial \gamma}{\partial x} dx\,,$$

where $n : \partial\Omega(x) \to \mathbb{R}^N$, $q \mapsto n(q)$ denotes the unit outward normal to $q \in \partial\Omega(x)$, and $\gamma : D \to \Omega(x)$, $D \subseteq \mathbb{R}^N$ denotes a parametrization of the family $\{\Omega(x) \subseteq \mathbb{R}^N \,|\, x \in D\}$ of star-shaped sets. Let $\bar{d}_{e_i}^{\mathrm{P}}(q, p_i) = d_{e_i}^{\mathrm{P}}(q, p_i)\phi(q)$. Using the Conservation of Mass law,

$$\begin{aligned}
\frac{\partial}{\partial p_j} \sum_{i=1}^{n} \int_{V_i^e} \bar{d}_{e_i}^{\mathrm{P}}(q, p_i)dq &= \\
\frac{\partial}{\partial p_j} \int_{V_j^e} \bar{d}_{e_j}^{\mathrm{P}}(q, p_j)dq &+ \sum_{i \in \mathcal{N}_j^e} \frac{\partial}{\partial p_j} \int_{V_i^e} \bar{d}_{e_i}^{\mathrm{P}}(q, p_i)dq \\
= \int_{V_j^e} \frac{\partial}{\partial p_j} \bar{d}_{e_j}^{\mathrm{P}}(q, p_j)dq &+ \int_{\partial V_j^e} \bar{d}_{e_j}^{\mathrm{P}}(q, p_j) n_j^t \frac{\partial \gamma_j}{\partial p_j} d\gamma_j \\
&+ \sum_{i \in \mathcal{N}_j^e} \int_{\partial V_i^e} \bar{d}_{e_i}^{\mathrm{P}}(q, p_i) n_i^t \frac{\partial \gamma_i}{\partial p_j} d\gamma_i\,.
\end{aligned}$$

Note that the boundary V_j^e is the union of planes Δ_{ij}^e, $i \in \mathcal{N}_j^e$, such that

$$\int_{\partial V_j^e} \bar{d}_{e_j}^{\mathrm{P}}(q, p_j) n_j^t \frac{\partial \gamma_j}{\partial p_j} d\gamma_j = \sum_{i \in \mathcal{N}_j^e} \int_{\Delta_{ij}^e} \bar{d}_{e_i}^{\mathrm{P}}(q, p_i) n_j^t \frac{\partial \gamma_j}{\partial p_j} d\gamma_j\,.$$

Note also that the normals $n_j = -n_i$ are constant along Δ_{ij}^e, and that $\bar{d}_{e_j}^{\mathrm{P}}(q, p_j) = \bar{d}_{e_i}^{\mathrm{P}}(q, p_i)$ when $q \in \Delta_{ij}^e$, $\forall\, i \in \mathcal{N}_j^e$. Then, we have that:

$$\int_{\partial V_j^e} \bar{d}_{e_j}^{\mathrm{P}}(q, p_j) n_j^t \frac{\partial \gamma_j}{\partial p_j} d\gamma_j + \sum_{i \in \mathcal{N}_j^e} \int_{\partial V_i^e} \bar{d}_{e_i}^{\mathrm{P}}(q, p_i) n_i^t \frac{\partial \gamma_i}{\partial p_j} d\gamma_i = 0\,.$$

and therefore,

$$\begin{aligned}
\frac{\partial}{\partial p_j} \sum_{i=1}^{n} \int_{V_i^e} \bar{d}_{e_i}^{\mathrm{P}}(q, p_i)dq &= \int_{V_j^e} \frac{\partial}{\partial p_j} \bar{d}_{e_j}^{\mathrm{P}}(q, p_j)dq \\
&= \int_{V_j^e} \frac{\partial}{\partial p_j} \left(\|q - p_j\|^2 + (E - E_j)\right) \phi(q)dq \\
&= 2 \int_{V_j^e} (p_j - q)\phi(q)dq = 2M_{V_j^e}(p_j - C_{V_j^e})\,.
\end{aligned}$$

The analysis of the partial derivatives with respect to E_i can be repeated in an analogous way. We have that:

$$\begin{aligned}
\frac{\partial}{\partial E_j} \sum_{i=1}^{n} \int_{V_i^e} \bar{d}_{e_i}^{\mathrm{P}}(q, p_i)dq &= \\
\int_{V_j^e} \frac{\partial}{\partial E_j} \left(\|q - p_j\|^2 + (E - E_j)\right) \phi(q)dq & \\
= -\int_{V_j^e} \phi(q)dq &= -M_{V_j^e}\,.
\end{aligned}$$

Therefore,

$$\mathcal{L}_X \mathcal{H}_e = \sum_{j=1}^{n} \Big(2M_{V_j^e}(p_j - C_{V_j^e})X_{p_j} - M_{V_j^e} X_{E_j} \Big)\,.$$

■

From equation (11) we clearly see that the terms $-M_{V_j^e} X_{E_j}$ are going to augment the value of the cost function as the energy content of each agent decreases. Similarly, any energy replenishing strategy will decrease the value of $\mathcal{H}_e$. Using Theorem 3 we can now state:

Proposition 4: Let the vector field X in (10) be defined by (9). Then the flow defined by X is a gradient descent algorithm for $\mathcal{H}_e$. Furthermore, the flow converges to the invariant set

$$\{(p_1, E_1, \dots, p_n, E_n) \in Q^n \times [0, E]^n \,| \; p_i = C_{V_i^e} \text{ or } E_i = 0,\ \forall i \in \{1, \dots, n\}\}\,.$$

Proof: The substitution of the dynamics for p_i and E_i into (11) lead to:

$$\mathcal{L}_X \mathcal{H}_e = \sum_{i=1}^{n} M_{V_i^e}(p_i - C_{V_i^e})\mathrm{sat}(p_i - C_{V_i^e})k(E_i)\left(-2 + k(E_i)\right)\,.$$

Observe that $\frac{d\mathcal{H}_e}{dt} \le 0$ since $(p_i - C_{V_i^e})\mathrm{sat}(p_i - C_{V_i^e}) \ge 0$ and $0 \le k(E_i) < 2$. The set of points (p_i, E_i) where $\mathcal{L}_X \mathcal{H}_e = 0$ is given by:

$$p_i(t) - C_{V_i^e}(t) = 0\,, \quad \text{or} \quad k(E_i)(t) = 0\,.$$

Since Q is a compact set, by LaSalle's invariance principle; see [15], the flow (9) will approach the largest invariant set contained in $\mathcal{L}_X \mathcal{H}_e = 0$. ∎

V. Simulations

In this section, we present comparisons of the performance of the different control laws proposed in the previous sections. In all simulations, we define $Q \subset \mathbb{R}^2$, where the vertices of Q are at $(0,0), (15,0), (12,10), (5,15), (0,10)$. We also consider a density function $\phi : Q \to \mathbb{R}_{\geq 0}$ given as $\phi(x_1, x_2) = \exp\left[-\frac{1}{9}\left((x_1-8)^2 + (x_2-8)^2\right)\right]$.

Starting from the same initial positions in all runs, the initial energy supply of 8 robotic agents is $E_i = 10$, $i \in \{1, \ldots, 4\}$ and $E_i = 2$ for $i \in \{5, \ldots, 8\}$. In addition, we assume agents become incapacitated when $E_i \leq 0.5$.

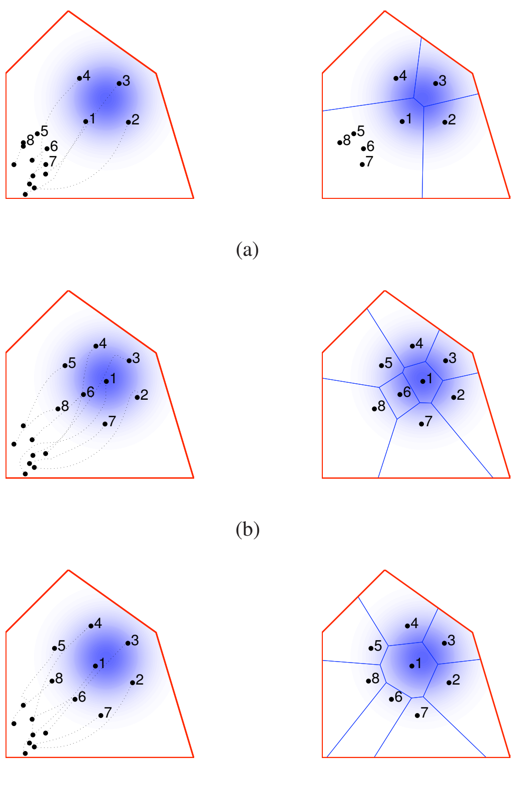

Fig. 2. Three simulation runs using law (7) (a), law (8) (b), law (9) (c).

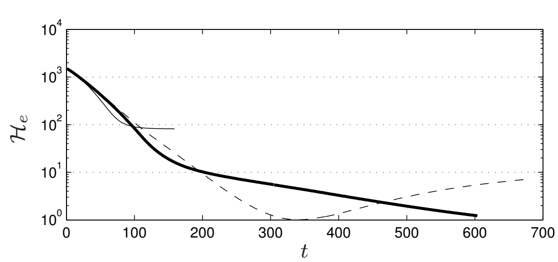

Fig. 3. Energy aware cost function evaluation using law (7) (light solid), law (8) (dashed), and law (9) (heavy solid). All costs are shifted such that the minimum cost of the three simulations is 1.

TABLE I
FINAL ENERGY AND ϕ-WEIGHTED AREAS OF DOMINANCE

	Law (7)		Law (8)		Law (9)	
Agent	E_i	Area	E_i	Area	E_i	Area
1	3.59	6.74	5.44	5.76	5.47	9.59
2	0.89	5.96	3.69	3.62	4.13	4.14
3	1.67	8.39	4.21	4.17	4.27	5.59
4	2.61	6.04	6.28	4.07	4.18	4.49
5	0.50	0.00	1.23	2.67	1.27	1.07
6	0.50	0.00	1.39	3.29	1.51	0.80
7	0.46	0.00	1.09	2.49	1.09	0.79
8	0.44	0.00	1.62	1.06	1.56	0.67

The simulation in Figure 2(a) illustrates failure of the four vehicles with low initial energy content. Because movement of agents is not dependent on energy, agents with little energy cease to function. Consequently, the remaining four vehicles must repartition the assigned region, increasing each agent's area of dominance.

The second simulation row in Figure 2(b) uses law (8), which allows the vehicles to expend energy proportional to their reserves. However, is not optimal in the power-aware sense as defined by (4). That is, the region of dominance of each agent takes no consideration of the energy content of neighbors, as is illustrated in the cost-function evaluation, Figure 3. The power-aware cost function, $\mathcal{H}_e$, increases along the flow evolution.

Observe that the graphs in Figure 3 have been plotted up to a time when agents have reached their final configurations (centroids) or their energy content becomes less or equal than 0.5.

The final simulation row in Figure 2(c) utilizes the full power-aware algorithm from (9). Through the use of power-aware partitions, $\mathcal{V}^e(P)$, as opposed to ordinary partitions, $\mathcal{V}(P)$, the resulting cost function $\mathcal{H}_e$ is minimized, as is stated by Proposition 4. The difference between the power weighted and ordinary Voronoi regions is revealed through the comparison of Figures 2(b) and 2(c), and Table I. Table I shows in detail the final energy content of each node with the area of its region of dominance. We can see (i) a more balanced energy consumption among the agents using law (9) and (ii) the area of the region of dominance of each agent better reflects their energy capacity. In particular, the sum of the areas for the agents $1, 2, 3, 4$ is larger with (9) than with (8). In general the final outcome depends strongly on the initial conditions. On average we have seen the behavior that we show here.

To explore the energy balancing in more detail, we include a simulation in 1D. In this simulation, four agents have the same initial positions, and varying initial energies. Agents $1, 2, 3, 4$ start at positions $3.3, 4.6, 5.1, 5.3$ with energies $15, 5, 2, 1$, respectively, and they must cover the region $q \in [0, 20]$, with $\phi(q) \equiv 1$.

The simulation shows the energy expenditure balancing that takes place to some extent using the power-aware scheme. Although energy expenditure might be higher in each node as compared with that as a result of law (8), we can observe a certain balancing that makes agents with

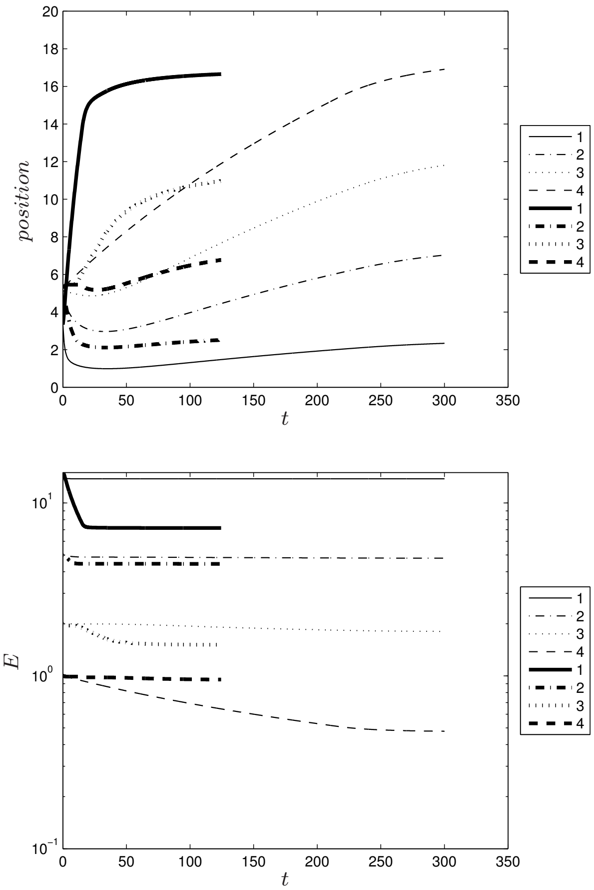

Fig. 4. 1D position and energy evolution comparison between law (8) (light lines) and law (9) (heavy lines) with agent numbers as indicated. Initial energy contents are $15, 5, 2, 1$ for agents $1, 2, 3, 4$ respectively.

lower energy spend less power using (9) than using (8). In this simulation, the node with least energy spends less at the cost of all other nodes spending more. The increased expenditure of power on each of the other agents is also explained by the fact that they have to move further to reach the centroids of their larger regions of dominance. The balancing is most noticeable when the initial energies satisfy $\max E_i(0) \gg \min E_i(0)$ for $i \in \{1, \ldots, n\}$. As with Figure 3, the graphs in Figure 4 have been plotted up to a time when either agents' positions have almost stabilized or $E \leq 0.5$.

VI. Conclusions and future work

We have presented new power-aware algorithms for coverage problems. We have introduced a new cost function that allows us to analyze and compare the performance of these algorithms. In particular, the second algorithm leads to a final configuration where agents with higher power are assigned regions with higher area.

More involved energy and vehicle dynamics are also a point of future research. In particular we will investigate the impact energy harvesting capabilities of vehicles due to, e.g., solar panels as well as developing gradient decent algorithms for nonholonomic dynamics.

VII. Acknowledgments

This material is based upon work supported by NSF Career Award CMS-0643673.

References

[1] S. Slijepcevic and M. Potkonjak, "Power efficient organization of wireless sensor networks," in *IEEE International Conference on Communications*, vol. 2, 2001, pp. 472–476.

[2] B. Chen, K. Jamieson, H. Balakrishnan, and R. Morris, "Span: an energy efficient coordination algorithm for topology maintenance in ad hoc wireless networks," *Wireless Networks*, vol. 8, no. 5, pp. 481–494, September 2002.

[3] F. Ye, G. Zhong, S. Lu, and L. Zhang, "PEAS: a robust energy conserving protocol for long-lived sensor networks," in *IEEE International Conference on Network Protocols*, 2002, pp. 200–201.

[4] V. Raghunathan, C. Pereira, M. Srivastava, and R. Gupta, "Energy-aware wireless systems with adaptive power-fidelity tradeoffs," *IEEE Trans. Very Large Scale Integration Systems*, vol. 13, no. 2, pp. 211–225, February 2005.

[5] S. Mohapatra, N. Dutt, A. Nicolau, and N. Venkatasubramanian, "DYNAMO: A cross-layer framework for end-to-end QoS and Energy Optimization in Mobile Handheld Devices," *IEEE J. Selected Areas in Communication*, May 2007.

[6] Y. Mei, Y. Lu, Y. Hu, and C. Lee, "Deployment strategy for mobile robots with energy and timing constraints," in *IEEE Int. Conf. on Robotics and Automation*, 2005, pp. 2816–2821.

[7] N. Heo and P. K. Varshney, "Energy-efficient deployment of intelligent mobile sensor networks," *IEEE Transactions on Systems, Man and Cybernetics, Part A*, vol. 35, no. 1, pp. 78–92, January 2005.

[8] Z. Sun and J. Reif, "On energy-minimizing paths on terrains for a mobile robot," in *IEEE Int. Conf. on Robotics and Automation*, vol. 3, 2003, pp. 3782–3788.

[9] W. Dunbar and R. Murray, "Distributed Receding Horizon control for Multi-Vehicle formation stabilization," *Automatica*, vol. 42, no. 4, pp. 549–558, 2006.

[10] Y. Kuwata, A. Richards, T. Schouwenaars, and J. How, "Distributed Robust Receding Horizon control for Multi- Vehicle guidance," *IEEE Trans. Control Systems Technology*, 2007, to appear.

[11] A. Okabe, B. Boots, K. Sugihara, and S. N. Chiu, *Spatial Tessellations: Concepts and Applications of Voronoi Diagrams*, 2nd ed., ser. Wiley Series in Probability and Statistics. New York: John Wiley, 2000.

[12] Z. Drezner, Ed., *Facility Location: A Survey of Applications and Methods*, ser. Springer Series in Operations Research. New York: Springer Verlag, 1995.

[13] J. Cortés, S. Martínez, and F. Bullo, "Spatially-distributed coverage optimization and control with limited-range interactions," *ESAIM. Control, Optimisation & Calculus of Variations*, vol. 11, pp. 691–719, 2005.

[14] J. Cortés, S. Martínez, T. Karatas, and F. Bullo, "Coverage control for mobile sensing networks," *IEEE Transactions on Robotics and Automation*, vol. 20, no. 2, pp. 243–255, 2004.

[15] H. K. Khalil, *Nonlinear Systems*, 2nd ed. Englewood Cliffs, NJ: Prentice Hall, 1995.